# Narrow-linewidth and stable-frequency light source for laser cooling of magnesium fluoride molecules

Yanning Yin, Yong Xia*, Xingjia Li, Xiuxiu Yang, Supeng Xu, and Jianping Yin

*State Key Laboratory of Precision Spectroscopy, Department of Physics, East China Normal University, Shanghai 200062, China*
E-mail: yxia@phy.ecnu.edu.cn

We demonstrate the frequency doubling, linewidth narrowing, and frequency stabilization of two cw Ti:sapphire lasers for the laser cooling of magnesium fluoride (MgF) molecules. From the energy-level structure of MgF, both lasers are frequency-doubled to ultraviolet to serve as cooling and repumping lasers. By constructively establishing a frequency stabilization system that firstly stabilizes both lasers via a "side-of-fringe" scheme to their reference resonators, which are then length-locked to a helium-neon (HeNe) laser through a transfer cavity, we obtain two lasers with a narrow linewidth of ~6 kHz and an extraordinary long-term frequency stability of ±2.8 MHz. © 2015 The Japan Society of Applied Physics

Tremendous progress has been made in laser cooling and the magnetooptical trapping of diatomic molecules,[1–5] which should hold promise for discoveries of new physics and chemistry, greatly facilitating research studies on precision measurement, strongly correlated many-body quantum systems, cold chemistry, and so forth.[6–8] Besides certain polar molecules (SrF, YO, CaF) that have been demonstrated, there are much more candidate molecules appropriate for laser cooling, such as the ongoing YbF,[9] BH,[10] CaH[11] and even polyatomic SrOH,[12] by virtue of quasicycling transitions with radiation wavelengths that can range from ultraviolet to infrared band, most of which necessitate a cw dye or a Ti:sapphire laser with a wide tunable wavelength range and adequate power. We have selected magnesium fluoride as a prototype molecule for laser cooling,[13] concerning primarily its two lowermost electronic states, namely, the ground state $X^2\Sigma^+$ and the excited state $A^2\Pi_{1/2}$. The transition $X^2\Sigma^+_{1/2}(v = 0, N = 1) \rightarrow A^2\Pi_{1/2}(v' = 0, J' = 1/2)$, with a lifetime of 7.2 ns, will be employed as the main transition at 359.3 nm for cycling and slowing. As highly diagonal Franck–Condon factors suppress the vibrational branching of $A^2\Pi_{1/2}$, only two additional lasers at 368.6 and 368.4 nm for repumping the $v = 1$ and 2 levels can limit the vibrational branching loss to $<10^{-6}$. Reference 14 has demonstrated the feasibility of using a PDH-locked reference cell and a transfer cavity to make the dye laser at 577 nm linewidth-narrowed and frequency-stabilized. However, a dye solution with a concentration of about 1 g/L (pyridine 1 in solvents of 10% ethylene glycol and 90% ethylene glycol phenyl ether) is used for a specific wavelength range (690–740 nm), yielding a dye laser with an efficiency of 8% for generating laser at 718 nm with a pump laser power of 12 W, which causes the power of the frequency-doubled laser at 359 nm to become too low to satisfy the basic requirement. Here, we demonstrate a newly prepared light source for the laser cooling of MgF with a commercial Ti:sapphire (Ti:S) laser (Matisse TS) that has a large tuning range (700–1030 nm) and a capacity for high-output laser power as a substitute for the dye model. We manipulate two Ti:S lasers by doubling their frequencies to ultraviolet to serve as cooling and repumping lights, narrowing their linewidths and stabilizing their frequencies, and measure the linewidth and long-term frequency stability of the settled laser on the basis of the beat note between them.

The integrated experimental setup is depicted in Fig. 1, consisting mainly of two sets of Ti:S lasers, each of which contains a cw pump laser (Millennia eV) and a laser head, two SF ("side-of-fringe") reference resonators, two frequency doublers, a HeNe laser, a transfer cavity, a DAQ card, and a PC with corresponding programs. As the spectral bandwidth of the laser generated in the laser head with Ti:S and an optical resonator covers a large wavelength range, the single-mode laser operation through various frequency-selective elements will be achieved through the following mechanism: The resonator mirrors with specific reflective coatings can initiatively filter out a certain range such as 700–780 nm. With a 1.7-m-long ring resonator allowing discrete resonances with frequencies separated by a spacing of ~160 MHz, the main broad-range tunable element, namely, a birefringent filter acting as a coarse bandpass filter with a free spectral range (FSR) of ~130 nm, narrows the frequency range down to ~50 GHz, which will be further restricted by a thin etalon with a FSR of 250 GHz and a quite small Finesse. A thick etalon (FSR: 20 GHz, Finesse: ~3) ensures that all except one desired longitudinal mode acquire so high losses that lasing becomes impossible. Without any active control, the output laser has a linewidth of ~20 MHz and a free-running frequency drift of >600 MHz/h.

The second-harmonic generation (SHG) process is performed in a commercial frequency doubler (WaveTrain) containing a resonator using the patented DeltaConcept design, composed of two cavity mirrors, a LBO crystal, and a prism attached with a PZT, through which the resonator length can be tracked according to the frequency variation of the incident laser by a servo loop based on the PDH stabilization method with EOM and other mode-matching optics, as shown in the doubler's optical layout in Fig. 1. The Brewster-cut 10-mm-long, 6-mm-wide, 4-mm-high crystal with a cutting angle $\theta$ of 90° with $\varphi = 36.3°$ is temperature-controlled at 35 °C in the resonator with a round-trip length of ~150 mm. The resonator with a triangular configuration has advantages in terms of relatively high doubling efficiency by employing a Brewster-angled prism and a crystal to reduce losses, favorable beam stability by using a lightweight prism that translates along the symmetry axis of the symmetric beam path for frequency tracking, and easy optics exchange for other wavelengths by just replacing the crystal and two resonator mirrors.

Equipping the two doublers with SHG crystals at specific wavelengths of 718 and 736 nm that satisfy our needs, we measure their doubling efficiency performance (Fig. 2), which indicates a quadratic relationship between the output
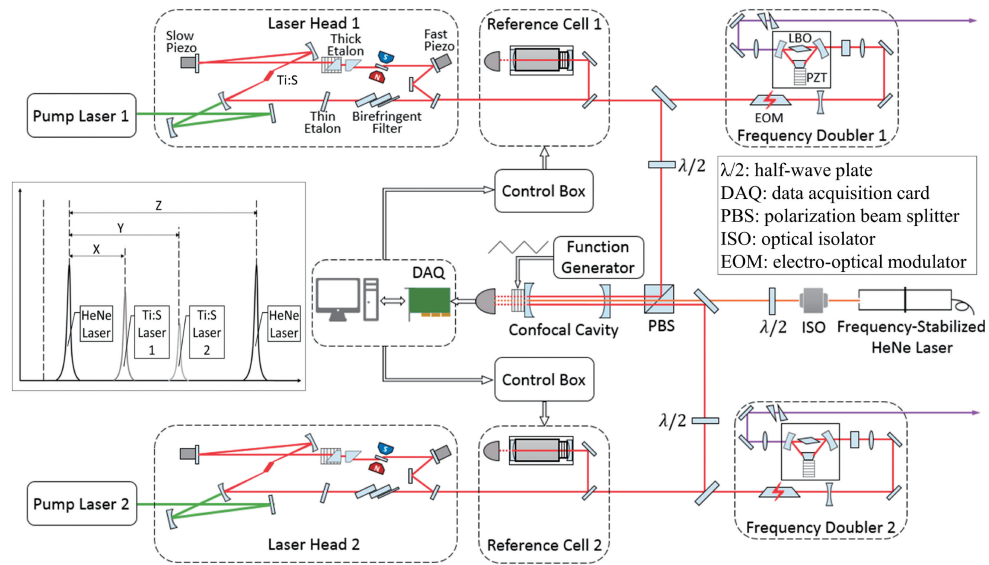
**Fig. 1.** Schematic of the experimental setup. The inset shows the transmission peaks of HeNe and two Ti:S lasers while scanning the transfer cavity. The peaks are set to different heights by adjusting half-wave plates to distinguish them.
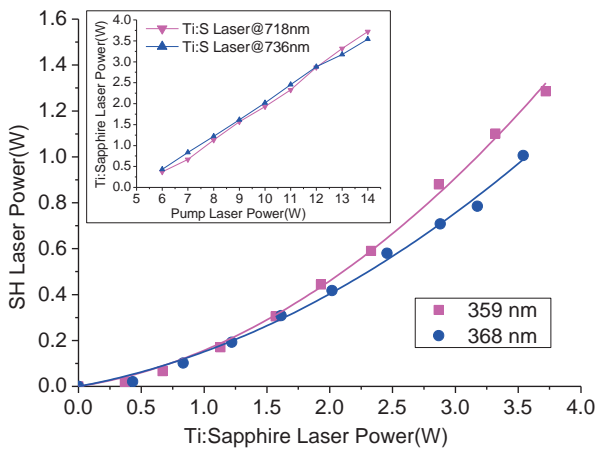


**Fig. 2.** Powers of SH lasers versus powers of Ti:S lasers. The circular and square dots are measured data, while the solid curves are quadratic fits. The inset shows the optimized powers of two Ti:S lasers versus the powers of their cw pump lasers, indicating an approximately linear relationship with the fitting $P_{Ti:S} = 0.4P_{Pump} - 2$.

SH power and the input fundamental power.[15,16] The inset of Fig. 2 also depicts the dependence of the power of the two Ti:S lasers from laser heads on the power of pump lasers, showing a linear relationship. A pump power of 14.0 W can lead to an input power ($P_{in}$) of 3.72 W at 718 nm ($P_{in}$ = 3.54 W at 736 nm) for the doubler and an output power ($P_{out}$) of 1.285 W at 359 nm ($P_{out}$ = 1.0 W at 368 nm). The maximum observed conversion efficiency is $\eta = P_{out}/P_{in} = 34.5\%$ for 359 nm (28.2% for 368 nm).

For some precision spectroscopy and molecular optics experiments, maintaining a highly frequency-stabilized and linewidth-narrowed laser is of such importance that many methods have been developed, including the PDH technique,[17] polarization locking,[18] and atomic or molecular transition line locking.[19] Our scheme takes advantage of a combination of two types of locking technique: SF scheme and transfer cavity method.[14,20] The former provides the narrowed linewidth and short-term stability, while the latter
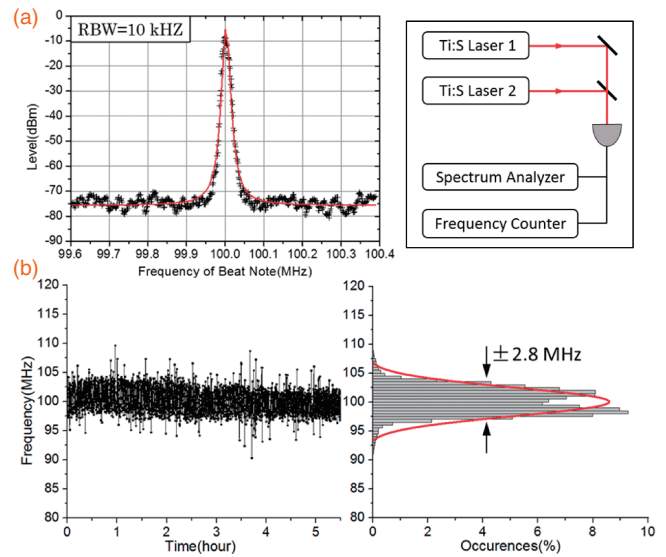
guarantees a long-term frequency locking. This type of stabilization scheme is particularly useful when no atomic or molecular reference lines are available and in the case that many stabilized lasers are required via one transfer cavity. As sketched in Fig. 1, the two Ti:S lasers are firstly locked to their respective vacuum-insulated and temperature-controlled reference cells with FSR of 600 MHz and Finesse of typically 15 to 20 by the so-called SF method, which intends to maintain laser frequency corresponding to a point of the flank of one of the reference cell's transmission resonances. Any tiny change in transmitted intensity due to laser frequency deviation relative to our set point will produce an error signal fed into a control loop consisting mainly of two actively controlled cavity mirrors mounted on Fast Piezo (to counteract relatively fast perturbations) and Slow Piezo (to ensure that Fast Piezo will always have its full dynamical range).

Locking to reference cells contributes to a narrowed laser linewidth and a short-term stabilization of laser frequency in comparison with the laser's free-running condition. However, this transient frequency stability has a drift of ∼74 MHz/h [Fig. 3(a)], which arises generally from a length creep of the reference cell owing to temperature fluctuation as well as piezo actuator relaxation. The transfer cavity method is utilized for eliminating these influences by locking the cell's length to a highly stable HeNe laser via a transfer cavity, so the long-term frequency stability of the HeNe laser (∼±2 MHz in 8 h) is transferred to the Ti:S laser. As also sketched in Fig. 1, a confocal, scanning Fabry–Perot interferometer (Toptica FPI100, FSR: 1.0 GHz, Finesse: 400) with mirrors covering 615–885 nm serving as a transfer cavity is injected with a combined beam comprising two Ti:S lasers and a HeNe beam, whose transmitted light through the cavity will be probed using a built-in photodetector as a scan is performed by exerting a triangular wave from a function generator on the PZT attached to one cavity mirror. The transmission signals that have been photoelectrically converted are visualized and processed via a DAQ card and a PC with the LabVIEW VI that we programmed. There are three
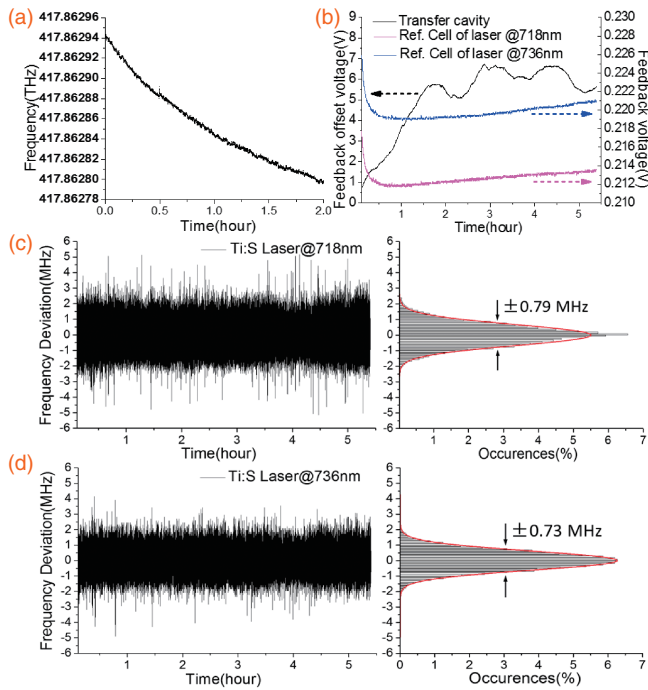
**Fig. 3.** (a) Typical frequency drift of Ti:S laser locked only to a reference cell. The data derived from the wavelength meter shows a drift rate of ~74 MHz/h. (b) Real-time feedback voltages applied to the transfer cavity (black line) and the reference cells of lasers at 718 nm (red line) and 736 nm (blue line). (c, d) Frequency deviations of stabilized lasers at 718 and 736 nm relative to that of the HeNe laser in more than 5 h and their statistic histograms. Relative frequency stabilities can be evaluated using the FWHM of Gaussian fitting curves.



**Fig. 4.** (a) Beat note of two stabilized Ti:S lasers with a frequency spacing of ~100 MHz, monitored using a spectrum analyzer with a RBW of 10 kHz. The inset sketches the setup for detecting the optical heterodyne beat note. (b) Frequency of beat note in more than 5 h, recorded using a frequency counter with an integration time of 100 ms, and its statistic histogram. The Gaussian fitting curve (red line) indicates a frequency stability of ~±2.8 MHz.

feedbacks in the VI: one is to lock the location of the HeNe transmission peak, while the other two serve to ensure fixed lengths of the reference cells in the case of drift. Firstly, by exploiting the real-time deviation of the HeNe laser's transmission peak location from our set point as an error, a corresponding voltage will be deduced through PI control algorithm and then as a bias added to the triangular wave for transfer cavity scanning; hence, the location of HeNe's peak is locked. Secondly, the DAQ card outputs two identical progressively increased voltages that will be imposed on the PZTs of the two reference cells through control boxes from 0 V to about half of the allowable maximum voltage of these PZTs at a so low speed that the two Ti:S lasers' initial locking to reference cells remains valid. Lastly, after computing the spacing of two adjacent HeNe peaks (denoted by $Z$ here, see the inset of Fig. 1) and the spacing between the HeNe peak and the first Ti:S laser peak (denoted by $X$), our program locks the ratio $X/Z$ onto a selected constant between 0 and 1 (denoted by $C_1$), by determining the error signal of $(X/Z - C_1)$ for another PI control that delivers a feedback voltage to the PZT of one reference cell as a correction of length drift, consequently realizing a long-term frequency locking of one Ti:S laser. As for another laser, we can just follow suit by similarly establishing a control loop that continuously compensates the difference between $Y/Z$ and another chosen constant $C_2$. It should be noted that in our experiments, both the frequency of the triangular wave for transfer cavity scanning and the sampling frequency of the DAQ card are set at 50 Hz, which proves to be optimal for stabilization results after our trials with different frequencies.

As can be inferred from our stabilization technique, the ultimate frequency stabilities of the desired Ti:S lasers depend basically on that of the HeNe laser, indicating that a better frequency reference laser source yields more favorable effects, so we firstly examine the two lasers' frequency deviations relative to that of the HeNe laser (denoted respectively by $\delta_1$ and $\delta_2$), which can be expressed as

$$\delta_1 = \left(\frac{X}{Z} - C_1\right) \times \frac{\lambda_{\text{ref}}}{\lambda_{\text{T1}}} \times \text{FSR},$$

$$\delta_2 = \left(\frac{Y}{Z} - C_2\right) \times \frac{\lambda_{\text{ref}}}{\lambda_{\text{T2}}} \times \text{FSR}, \quad (1)$$

where $\lambda_{\text{ref}}$, $\lambda_{\text{T1}}$, and $\lambda_{\text{T2}}$ are the wavelengths of the HeNe laser and two Ti:S lasers, respectively, and FSR represents the free spectral range of the transfer cavity. Acquiring the data of frequency deviations directly from our program, we can obtain the relative frequency stabilities of the two lasers [Figs. 3(c) and 3(d)], which can be evaluated as ±0.79 and ±0.73 MHz through histogram statistics and Gaussian curve fitting. Real-time data of feedback voltages imposed on the PZTs of the transfer cavity as well as on two reference cells are also exported from the VI and depicted in Fig. 3(b), which can help us understand the process of control loops and ambient influences.

For an exploration of the absolute frequency stabilities and the linewidths of the two settled lasers, the optical heterodyne beat note between them is recorded and analyzed, as sketched in the inset of Fig. 4, by tuning the two stabilized lasers to close frequencies (100 MHz, for example) and superimposing the beams into a home-made detector with a silicon PIN photodiode based on two-stage amplification, whose AC signals will be monitored using a spectrum analyzer and a frequency counter. With a resolution bandwidth (RBW) of 10 kHz, the spectrum of the beat note and its Lorentz fitting are shown in Fig. 4(a) and it reveals a linewidth of 12 kHz, which

**Table I.** Parameters of lasers under different conditions.

|  | Frequency drift | Linewidth |
|---|---|---|
| Free running | >600 MHz/h | ~20 MHz |
| Locked to ref. cell | ~74 MHz/h | 6 kHz |
| SF and transfer cavity scheme | ~±2.8 MHz/h | 6 kHz |

indicates that the stabilized laser reaches a significantly narrowed linewidth of 6 kHz on the assumption that the two lasers have identical linewidths. Furthermore, as shown in Fig. 4(b), a continuous observation of more than 5 h through the counter indicates that the beat note has a long-term frequency stability of ±2.8 MHz, which should result from a joint effect of the relative stabilities of Ti:S lasers and the stability of the HeNe laser with fluctuations within ±2 MHz; thus, we believe that a more stabilized frequency reference source can contribute to better stabilization results. Allowing for the Allan deviation of the beat note and the average nominal frequency of the two lasers, we can accordingly estimate the absolute frequency stability represented by the Allan standard deviation of either Ti:S laser to be $8.5 \times 10^{-10}$ with an integration time of 100 ms, which should manifest the desirable effectiveness of our frequency stabilization method. For an intuitive comparison of the lasers with and without our digital signal processing, we list some relevant parameters in Table I.

In conclusion, we have presented the preliminary experimental preparations of two Ti:S lasers serving respectively as cooling and repumping lasers in the laser cooling of molecular MgF beams, including frequency doubling, linewidth narrowing, and long-term frequency stabilization. The optimized efficiency performance characteristics of the two Ti:S lasers as well as the frequency doublers are all checked out, and the results prove to be satisfactory in our demand for laser power. Along with a constructive frequency stabilization scheme that takes advantage of the beneficial characteristics of two types of stabilization method, namely, transfer cavity stabilizing and "side-of-fringe" locking, we have obtained two feasible ultraviolet lasers with a narrow linewidth of ~6 kHz and a long-term frequency stability of ±2.8 MHz, which will be adequate for the laser cooling of MgF with a natural linewidth of the main transition estimated at $2\pi \times 22$ MHz.

We emphasize here that this stabilization scheme highlights the superiority of giving consideration to both long-term frequency locking and the capacity of locking to an arbitrary tunable frequency as we desire, and it can also be extended to three or more Ti:S or other types of laser to realize their simultaneous frequency stabilization, especially when there are no atomic or molecular reference lines available for locking. Although some groups, especially working in the field of cold atoms, have achieved frequency (or even phase) stabilization of two lasers with a frequency comb system,[3] in comparison with their relatively complicated comb system, the robust and versatile solution demonstrated here for locking the Ti:S (or diode, dye) lasers is more accessible and particularly useful for applications in the laser cooling of molecules, which need linewidth-narrowed and frequency-stabilized lasers. By further steps of optical modulation and chirping, these lasers should play crucial roles in our laser cooling experiments.

1) E. S. Shuman, J. F. Barry, D. R. Glenn, and D. DeMille, Phys. Rev. Lett. **103**, 223001 (2009).
2) E. S. Shuman, J. F. Barry, and D. DeMille, Nature **467**, 820 (2010).
3) M. T. Hummon, M. Yeo, B. K. Stuhl, A. L. Collopy, Y. Xia, and J. Ye, Phys. Rev. Lett. **110**, 143001 (2013).
4) V. Zhelyazkova, A. Cournol, T. E. Wall, A. Matsushima, J. J. Hudson, E. A. Hinds, M. R. Tarbutt, and B. E. Sauer, Phys. Rev. A **89**, 053416 (2014).
5) J. F. Barry, D. J. McCarron, E. B. Norrgard, M. H. Steinecker, and D. DeMille, Nature **512**, 286 (2014).
6) J. Doyle, B. Friedrich, R. V. Krems, and F. Masnou-Seeuws, Eur. Phys. J. D **31**, 149 (2004).
7) L. D. Carr, D. DeMille, R. V. Krems, and J. Ye, New J. Phys. **11**, 055049 (2009).
8) D. S. Jin and J. Ye, Chem. Rev. **112**, 4801 (2012).
9) I. J. Smallman, F. Wang, T. C. Steimle, M. R. Tarbutt, and E. A. Hinds, J. Mol. Spectrosc. **300**, 3 (2014).
10) R. J. Hendricks, D. A. Holland, S. Truppe, B. E. Sauer, and M. R. Tarbutt, Front. Phys. **2**, 51 (2014).
11) J. Velasquez, III and M. Di Rosa, Proc. Int. Symp. Molecular Spectroscopy, 2014.
12) I. Kozyryev, L. Baum, K. Matsuda, P. Olson, B. Hemmerling, and J. M. Doyle, New J. Phys. **17**, 045003 (2015).
13) D. P. Dai, Y. Xia, Y. F. Fang, L. Xu, Y. N. Yin, X. J. Li, X. X. Yang, and J. P. Yin, J. Phys. B **48**, 085302 (2015).
14) D. P. Dai, Y. Xia, Y. N. Yin, X. X. Yang, Y. F. Fang, X. J. Li, and J. P. Yin, Opt. Express **22**, 28645 (2014).
15) G. D. Boyd and D. A. Kleinman, J. Appl. Phys. **39**, 3597 (1968).
16) N. Chiodo, F. Du-Burck, J. Hrabina, M. Lours, E. Chea, and O. Acef, Opt. Lett. **39**, 2936 (2014).
17) R. W. P. Drever, J. L. Hall, F. V. Kowalski, J. Hough, G. M. Ford, A. J. Munley, and H. Ward, Appl. Phys. B **31**, 97 (1983).
18) T. W. Hansch and B. Couillaud, Opt. Commun. **35**, 441 (1980).
19) M. Zhu and J. L. Hall, in *Experimental Methods in the Physical Sciences*, ed. F. B. Dunning and R. G. Hulet (Academic Press, New York, 1997) Vol. 29, Part C, p. 103.
20) E. Riedle, S. H. Ashworth, J. T. Farrell Jr., and D. J. Nesbitt, Rev. Sci. Instrum. **65**, 42 (1994).